

Nanoscale Dynamics of Phase Flipping in Water near its Hypothesized Liquid-Liquid Critical Point

T. A. Kesselring,^{1,*} G. Franzese,² S. V. Buldyrev,³ H. J. Herrmann,^{1,4} and H. E. Stanley⁵

¹*Computational Physics, IfB, ETH Zurich,
Schafmattstrasse 6, 8093 Zurich, Switzerland*

²*Departament de Física Fonamental, Universitat de Barcelona,
Diagonal 645, 08028 Barcelona, Spain*

³*Department of Physics, Yeshiva University,
500 West 185th Street, New York, NY 10033*

⁴*Departamento de Física, Universidade Federal do Ceará,
Campus do Pici, 60451-970 Fortaleza, Ceará, Brazil*

⁵*Center for Polymer Studies and Department of Physics,
Boston University, Boston, MA 02215*

(Dated: Submitted 8 December 2011)

PACS numbers:

*Electronic address: tobiaskesselring@ethz.ch

Achieving a coherent understanding of the many thermodynamic and dynamic anomalies of water is among the most important unsolved puzzles in physics, chemistry, and biology. One hypothesized explanation imagines the existence of a line of first order phase transitions separating two liquid phases and terminating at a novel “liquid-liquid” critical point in a region of low temperature ($T \approx 250\text{K}$) and high pressure ($P \approx 200\text{MPa}$). Here we analyze a common model of water, the ST2 model, and find that the entire system flips between liquid states of high and low density. Further, we find that in the critical region crystallites melt on a time scale of nanoseconds. We perform a finite-size scaling analysis that accurately locates both the liquid-liquid coexistence line and its associated liquid-liquid critical point.

We perform extensive molecular dynamics (MD) simulations of ST2-water in the constant-temperature, constant-pressure ensemble. A typical example of $N = 343$ molecules at $P = 215 \text{ MPa}$ and $T = 244 \text{ K}$ exhibits phase flipping between low density liquid (LDL) and high density liquid (HDL) over a huge range of time scales, ranging from $\approx 20\text{ns}$ to $\approx 1 \mu\text{s}$ (Fig. 1), consistent with small-angle X-ray scattering studies [1, 2]. This nanoscale phase flipping results in a bimodal density distribution (Fig. 1(b)) and is observed for all temperatures and pressures in a region around the liquid-liquid (LL) phase transition that shrinks with growing system size.

As described in the *Methods* section, we equilibrate the system for times ranging from $\approx 100\text{ns}$ to $1 \mu\text{s}$ for 100 state points in the supercooled liquid region of water. The pressure ranges from 190 MPa to 240 MPa and temperatures are as low as 230 K at high P or 244 K at low P [Fig. 2(a)]. We consider four system sizes, $N = 216, 343, 512,$ and 729 molecules. We average over up to eleven independent runs for each state point. Using the histogram reweighting method [3], we interpolate our data along isobars.

To ensure that the system is in thermal equilibrium, we calculate the correlation time for the first maximum k_1 of the oxygen-oxygen intermediate scattering function $S_{OO}(k, t)$ [4] (as defined in the *Methods* section). While correlation times in the HDL phase are very short ($\approx 0.01 \text{ ns}$), they become of the order of 100 ns in the LDL phase at high enough T (see Fig. 3), implying that simulations of less than $1 \mu\text{s}$ are likely affected by poor statistical sampling.

We find that for $P \gtrsim 200 \text{ MPa}$ the density ρ decreases sharply within a narrow temper-

ature range while at lower P it falls off with T continuously. This behavior is consistent with a high- P discontinuous phase transition that ends in a LL critical point at lower P . This LL critical point was originally hypothesized [5] based on studies of the ST2 model, and subsequently studied in detail by many others using, in addition to ST2 [6, 7] a wide variety of different intermolecular potentials—such as TIP4P-Ew [8] and TIP4P/2005 [9], and coarse-grained models [10]. The existence of the LL critical point is also used to understand X-ray spectroscopy results [11] and hysteresis effects [12]. A strong indicator that a discontinuous phase transition is present is the bimodal density distribution that is related to the phase flipping studied here (Fig. 1).

Abrupt changes in the global density ρ are related to the appearance of different local structures. Among various parameters describing the local structures (see *Methods* section) we identified $q_6^{(2)}$ as being the best to distinguish the LDL and HDL phases. The fact that $q_6^{(2)}$ is defined over the second coordination shell of each molecule is consistent with structural characterizations based on experiments [13] showing that in supercooled water the two locally coexisting structures mainly differ in their second shells. Nevertheless, with a few exceptions such as those discussed in Refs. [14] and [15], most previous studies of supercooled water have focused on analyzing only the structural differences at the first coordination shell.

The average values of $q_6^{(2)}$ of the two phases differ by about 15%, the LDL phase being characterized by greater order in the second shell than in the HDL phase [Fig. 1(c) and (d)]. The distributions of $q_6^{(2)}$ for individual molecules in the two phases partially overlap, since $q_6^{(2)}(\text{HDL}) = 0.25 \pm 0.05$ and $q_6^{(2)}(\text{LDL}) = 0.30 \pm 0.06$.

To show that the LL phase transition exists in the thermodynamic limit, we perform a finite-size analysis for the bimodality of the density distribution function, $p(\rho)$, along isobars within the supercooled liquid region. For that purpose, we consider the Challa-Landau-Binder parameter $\Pi = 1 - \frac{\langle \rho^4 \rangle}{3\langle \rho^2 \rangle^2}$ [16, 17]. When $p(\rho)$ is unimodal, Π adopts the value $2/3$ in the thermodynamic limit $N \rightarrow \infty$, while $\Pi < 2/3$ when $p(\rho)$ is bimodal, i.e. two phases coexist.

However, for a finite system $\Pi < 2/3$ whenever $p(\rho)$ deviates from a delta function. This occurs where the isothermal compressibility, κ_T , has maxima, i.e., along a locus in the P - T plane that includes (i) the discontinuous phase transition at $P > P_C$, (ii) the effective LL critical point at $P_C(N)$, where the discontinuity vanishes, and (iii) a line at $P < P_C$ that

emanates from the LL critical point into the supercritical region. This line follows the locus of maxima of the correlation length, known as the Widom line [18, 19].

The finite-size behavior of Π allows to discriminate if an isobar is above or below P_C [16, 17] (Fig. 2 b). When isobars cross the Widom line ($P < P_C$), Π displays a minimum Π_{\min} that in leading order approaches $2/3$ linearly with $1/N$. When $p(\rho)$ consists of two Gaussians of equal weight, i.e. at the coexistence line for $P \gtrsim P_C$, Π_{\min} approaches, also linearly with $1/N$, another limiting value $\Pi \rightarrow 1 - 2(\rho_P(\text{HDL})^4 + \rho_P(\text{LDL})^4) / [3(\rho_P(\text{HDL})^2 + \rho_P(\text{LDL})^2)^2]$ where $\rho_P(\text{HDL})$ and $\rho_P(\text{LDL})$ are the densities of the two coexisting phases [16]. This limiting value progressively decreases with $P > P_C$ because $\rho_P(\text{HDL})$ and $\rho_P(\text{LDL})$ at coexistence increase. Therefore Π allows us to precisely identify the region within which the LL critical point is located.

To estimate the critical exponents of the LL critical point we next investigate the distribution of the order parameter M of the LL phase transition. As for the liquid-gas phase transition [20], the order parameter is not simply the density, but a linear combination of the density with another observable [21]. Here we choose the linear combination of density and energy $M \equiv \rho + sE$ [20] and find that it follows, as expected, the behavior of a liquid in the universality class of the three dimensional Ising model, as it is also the case for the liquid-gas transition. This is shown in Fig. 4a for $N=343$ molecules. At $P = 205$ MPa the difference between the maxima and the central minimum of the order parameter distribution is smaller than for the three dimensional Ising case. At $P = 210$ MPa it is larger and the critical point therefore seems to be in between, consistent with the conclusion obtained before analyzing Π . We get the best fit of the order parameter distribution function at a pressure of $P = 206 \pm 3$ MPa and a temperature of $T = 246 \pm 1$ K.

The same analysis for $N = 512$ and 729 gives an estimate of the LL critical point at 208 ± 3 MPa and 246 ± 1 K consistent with $N = 343$ (4 b and c). The finite size scaling of the amplitudes of the order parameter distribution $A \sim L^{\beta/\nu}$ is consistent with the behavior predicted for the three dimensional Ising universality class with $\beta/\nu \approx 0.518$ [20] and strong corrections to scaling for $N \lesssim 343$ as seen in Fig. 4d.

Finally, we investigate also the possibility of spontaneous crystal nucleation in the LDL phase using the structural order parameter d_3 Ref. [22] (defined in the *Methods* section). At temperatures below the region of phase flipping, the samples sometimes form large crystallites filling up to 10% of the systems volume. Their structure exhibits a mixture of cubic

and hexagonal symmetry. However, in approximately 99% of cases these unstable crystallites melt again within the simulation time of $1\mu\text{s}$ (Fig. 5), showing that the free-energy barrier for the crystallization process is significantly larger than $k_B T$ in the LDL phase. We observe irreversible crystallization in only 3 out of 350 $1\mu\text{s}$ runs all of which correspond to state points near the LL transition line (Fig. 2 a), consistent with the general result that a metastable fluid-fluid phase transition favors crystallization process in its vicinity [23]. Therefore, the LDL seems to be a genuine metastable phase with respect to the stable crystal phase.

In conclusion, we investigate in new ways both the statics and dynamics of deeply supercooled ST2-water. Specifically we analyze static calculations using the framework of finite-size scaling theory, and we analyze dynamic calculations over three orders of magnitude of time scales, from 1 ns to 1000 ns. We find definitive evidence of a first order LL phase transition line between two genuine metastable phases. The phase transition line terminates in a LL critical point, and the exponents associated with this LL critical point are indistinguishable from those expected for a lattice-gas model which is known to describe the liquid-vapor critical point.

After this work was underway, we learned that other groups, using different approaches, are addressing the question of the hypothesized existence of a LL phase transition line and the associated LL critical point. We are grateful to Y. Liu, A. Z. Panagiotopoulos, P. Debenedetti, F. Sciortino, I. Saika-Voivod, P. H. Poole, D. T. Limmer and D. Chandler for sharing their results. Our results agree with the very recent work of Sciortino, Poole and Saika-Voivod [24, 25] and with Liu and Debenedetti et al, working along similar lines (P. G. Debenedetti, private communication) but not with the conclusions of Ref. [26].

We thank S.-H. Chen, P. H. Poole, and F. Sciortino for a critical reading of the manuscript and for helpful suggestions. GF thanks Ministerio de Ciencia e Innovación-Fondo Europeo de Desarrollo Regional (Spain) Grant FIS2009-10210 for support. SVB acknowledges the partial support of this research through the Dr. Bernard W. Gamson Computational Science Center at Yeshiva College and through the Departament d'Universitats, Recerca i Societat de la Informació de la Generalitat de Catalunya. HES thanks the NSF Chemistry Division for support (grants CHE 0911389 and CHE 0908218).

I. METHODS

We performed MD simulations in the NPT ensemble using the five-point water model ST2 of Stillinger and Rahman [27] consisting of five particles interacting through electrostatic and Lennard-Jones forces with a cutoff of 7.8 Å. The pressure was not adjusted to correct for the effects of the Lennard-Jones cutoff, since they would originate from mean field calculations, which become rather poor near a critical point.

We apply the Shake algorithm to constrain the particles inside each molecule. The constant pressure is imposed by a barostat, and a Nosé-Hoover thermostat is applied to ensure constant temperature [28]. Periodic boundary conditions have been implemented.

For the simulations we used the following protocol consisting of three steps: (1) For a chosen initial density first a constant volume simulation is performed at $T = 300$ K during 1 ns (first pre-run). (2) The ensemble is then changed to NPT by adding the Berendsen barostat and the temperature is reduced to $T = 265$ K, ensuring that the system reaches the HDL phase after 1 ns of equilibration. (3) After these two pre-runs the system is quenched to the final pressure and temperature, from which the first 100 – 200 ns are removed as thermalization time. The choice of the thermalization time will be discussed next.

To decide if the equilibration time is sufficient, we perform two steps. First, we inspect the time series of energy and density to discard the possibility of spontaneous crystallization. In all our NPT simulations we observed only three crystallization events all of them in systems of 343 molecules. We use them as a reference for the crystal. In a second step we measure the correlation time using the intermediate scattering function.

The order parameter $M = \rho + sE$ is obtained from the distribution in the density - energy plane (Fig. 4 e), by integrating it with a delta-function $\delta(M - \rho - sE)$. We select the value of s for which the distribution of M fits best the distribution of the order parameter for the 3d Ising universality class. The main effect found when changing s is a small shift in the estimated critical temperature T_c of about 0.1 K which is less than the error of 0.5 K originating from the histogram reweighting.

The intermediate scattering function $S(\vec{k}, t)$ can be used to distinguish between phases of different structure as LDL and HDL. We also use it to estimate the correlation time. It

is defined as [4]

$$S(\vec{k}, t) = \frac{1}{N} \left\langle \sum_{l,m}^N \exp(i\vec{k} [\vec{r}_l(t) - \vec{r}_m(t)]) \right\rangle, \quad (1)$$

$\vec{r}_l(t)$ is the position of particle l at time t , \vec{k} the wave vector and k its magnitude $|\vec{k}|$. $S(\vec{k}, t)$ describes the time evolution of the spatial correlation along the wave vector \vec{k} . We also use this intermediate scattering function to calculate the correlation specifically between the O atoms calling it then $S_{OO}(k)$. With the intermediate scattering function we compute the correlation time defined as

$$C_{OO}(k, \tau) = \frac{\langle (S_{OO}(k, t) - \langle S_{OO}(k, t) \rangle_t) \times (S_{OO}(k, t + \tau) - \langle S_{OO}(k, t + \tau) \rangle_t) \rangle_t}{\langle S_{OO}(k, t) - \langle S_{OO}(k, t) \rangle_t \rangle_t^2},$$

where $\langle . \rangle$ stands for the average over time t . As k we chose the vector from the first three maxima of $\langle S_{OO}(k, t) \rangle_t$ for which $C_{OO}(k, \tau)$ decays slowest. We define the correlation time as the time after which this function falls below $1/e$ (Fig. 3). We find for instance $\tau < 0.001$ ns at $T = 251$ K and $P = 200$ MPa or at $T = 240$ K and $P = 240$ MPa .

We use the order parameter q_6 as defined in Ref. [22]. For this purpose we first define

$$q_{l,m}^i = \frac{1}{4} \sum_{j \in n_i}^4 Y_l^m(\varphi_{ij}, \vartheta_{ij}), \quad -l \leq m \leq l$$

where $Y_l^m(\varphi_{ij}, \vartheta_{ij})$ are the l, m spherical harmonic functions for the polar angles φ_{ij} and ϑ_{ij} , of the bond between particles i and j relative to an arbitrary coordination system. n_i is the set containing all next nearest neighbors of molecule i (second coordination shell). We define as the first shell the four nearest neighbors and as the second shell the sixteenth nearest neighbors that are not in the first shell. To distinguish the two different shells we add a subscript, hence writing $q_6^{(2)}$ for q_6 calculated in the second shell.

The local order parameter q_l is defined using the above definition of $q_{l,m}^i$, averaged over the particles i and summed over all m :

$$q_l = \frac{1}{N} \sum_i \sum_m q_{l,m}^i \quad (2)$$

where N is the number of particles. We use $l = 6$.

The bond based order parameter d_3 as defined in Ref. [29] is designed to distinguish between a fluid and a diamond structure. It uses the Y_{3m} spherical harmonics to identify the tetragonal symmetry of the diamond structure. To define d_3 one needs $q_{3,m}(i)$:

$$q_{3,m}(i) = \frac{1}{Z_i} \sum_{i \neq j} (r_{ij}) Y_{3m} \left(\frac{\vec{r}_{ij}}{|r_{ij}|} \right) \quad (3)$$

where the sum goes over the first four nearest neighbors and Z_i is the fractional number of neighbors. Normalizing this quantity results in

$$q'_{3,m}(i) = \frac{q_{3,m}(i)}{\left(\sum_{m=-l}^l q_{3,m}(i)q_{3,m}^*(i)\right)^{1/2}}. \quad (4)$$

where $q_{3,m}^*(i)$ is the complex conjugate of $q_{3,m}$. This normalized quantity is then used to define

$$d_{3,m}(i) = \sum_{m=-l}^l q'_{3,m}(i)q_{3,m}^*(j), \quad (5)$$

-1 and 1 being -1 for a perfect structure of both diamond or graphite. As in Ref [29], we consider two particles to be connected with a graphite or diamond bond if $d_3(i, j) \leq d_c = -0.87$ and a molecule is considered to belong to a crystal if three out of four bonds satisfy this condition (Fig. 5).

-
- [1] Huang, C. *et al.* The inhomogeneous structure of water at ambient conditions. *Proc Nat Acad Sci USA* **106**, 15214–8 (2009).
- [2] Wikfeldt, K. T., Nilsson, A. & Pettersson, L. G. M. Spatially inhomogeneous bimodal inherent structure of simulated liquid water. *Phys. Chem. Chem. Phys.* **13**, 19918–24 (2011).
- [3] Panagiotopoulos, A. Z. Monte Carlo methods for phase equilibria of fluids. *J. Phys.: Condens. Matter* **12**, 25–52 (2000).
- [4] Franzese, G., Malescio, G., Skibinsky, A., Buldyrev, S. V. & Stanley, H. E. Metastable liquid-liquid phase transition in a single-component system with only one crystal phase and no density anomaly. *Phys. Rev. E* **66**, 051206 (2002).
- [5] Poole, P., Sciortino, F., Essmann, U. & Stanley, H. Phase-behavior of metastable water. *Nature* **360**, 324–328 (1992).
- [6] Poole, P. H., Saika-Voivod, I. & Sciortino, F. Density minimum and liquid-liquid phase transition. *J. Phys.: Condens. Matter* **17**, L431–L437 (2005).
- [7] Liu, Y., Panagiotopoulos, A. Z. & Debenedetti, P. G. Low-temperature fluid-phase behavior of ST2 water. *J. Chem. Phys.* **131**, 104508 (2009).
- [8] Paschek, D., Ruppert, A. & Geiger, A. Thermodynamic and structural characterization of the transformation from a metastable low-density to a very high-density form of supercooled TIP4P-Ew model water. *ChemPhysChem* **9**, 2737–2741 (2008).
- [9] Abascal, J. L. F. & Vega, C. Widom line and the liquid–liquid critical point for the TIP4P/2005 water model. *J. Chem. Phys.* **133**, 234502 (2010).
- [10] Franzese, G., Marqués, M. I. & Stanley, H. E. Intramolecular coupling as a mechanism for a liquid-liquid phase transition. *Phys. Rev. E* **67**, 011103 (2003).
- [11] Nilsson, A. & Pettersson, L. G. M. Perspective on the structure of liquid water. *Chem. Phys.* **389**, 1–34 (2011).
- [12] Zhang, Y. *et al.* Density hysteresis of heavy water confined in a nanoporous silica matrix. *Proc Nat Acad Sci USA* **108**, 12206–12211 (2011).
- [13] Soper, A. & Ricci, M. Structures of high-density and low-density water. *Phys. Rev. Lett.* **84**, 2881–2884 (2000).
- [14] Saitta, A. M. & Datchi, F. Structure and phase diagram of high-density water: The role of

- interstitial molecules. *Phys. Rev. E* **67**, 020201 (2003).
- [15] Yan, Z. *et al.* Structure of the first- and second-neighbor shells of simulated water: Quantitative relation to translational and orientational order. *Phys. Rev. E* **76**, 051201 (2007).
- [16] Challa, M. S. S., Landau, D. P. & Binder, K. Finite-size effects at temperature-driven first-order transitions. *Phys. Rev. B* **34**, 1841–1852 (1986).
- [17] Franzese, G. Potts fully frustrated model: Thermodynamics, percolation, and dynamics in two dimensions. *Phys. Rev. E* **61**, 6383–6391 (2000).
- [18] Xu, L. *et al.* Relation between the Widom line and the dynamic crossover in systems with a liquid-liquid phase transition. *Proc Nat Acad Sci USA* **102**, 16558–16562 (2005).
- [19] Franzese, G. & Stanley, H. E. The Widom line of supercooled water. *J. Phys.: Condens. Matter* **19**, 205126 (2007).
- [20] Wilding, N. B. Simulation studies of fluid critical behaviour. *J. Phys.: Condens. Matter* **585**, 585–612 (1997).
- [21] Bertrand, C. E. & Anisimov, M. A. Peculiar thermodynamics of the second critical point in supercooled water. *J. Phys. Chem. B* **115** (2011).
- [22] Steinhardt, P. J., Nelson, D. R. & Ronchetti, M. Bond-orientational order in liquids and glasses. *Phys. Rev. B* **28**, 784–805 (1983).
- [23] tenWolde, P. R. & Frenkel, D. Enhancement of protein crystal nucleation by critical density fluctuations. *Science* **277**, 1975–1978 (1997).
- [24] Poole, P. H., Becker, S. R., Sciortino, F. & Starr, F. W. Dynamical behavior near a liquid-liquid phase transition in simulations of supercooled water. *J. Phys. Chem. B* **115**, 14176–14183 (2011).
- [25] Sciortino, F., Saika-Voivod, I. & Poole, P. H. Study of the ST2 model of water close to the liquid-liquid critical point. *Phys. Chem. Chem. Phys.* **13**, 19759–64 (2011).
- [26] Limmer, D. T. & Chandler, D. The putative liquid-liquid transition is a liquid-solid transition in atomistic models of water. *J. Chem. Phys.* **135**, 134503 (2011).
- [27] Stillinger, F. & Rahman, A. Improved simulation of liquid water by molecular-dynamics. *J. Chem. Phys.* **60**, 1545–1557 (1974).
- [28] Allen, M. P. & Tildesley, D. J. *Computer Simulation of Liquids*. Oxford Science Publications (Oxford University Press, 1987).
- [29] Ghiringhelli, L. M. *et al.* State-of-the-art models for the phase diagram of carbon and diamond

nucleation. *Mol. Phys.* **106**, 2011–2038 (2008).

- [30] Hilfer, R. & Wilding, N. B. Are critical finite-size scaling functions calculable from knowledge of an appropriate critical exponent? *J. Phys. A-Math. Gen.* **28**, 281–286 (1995).

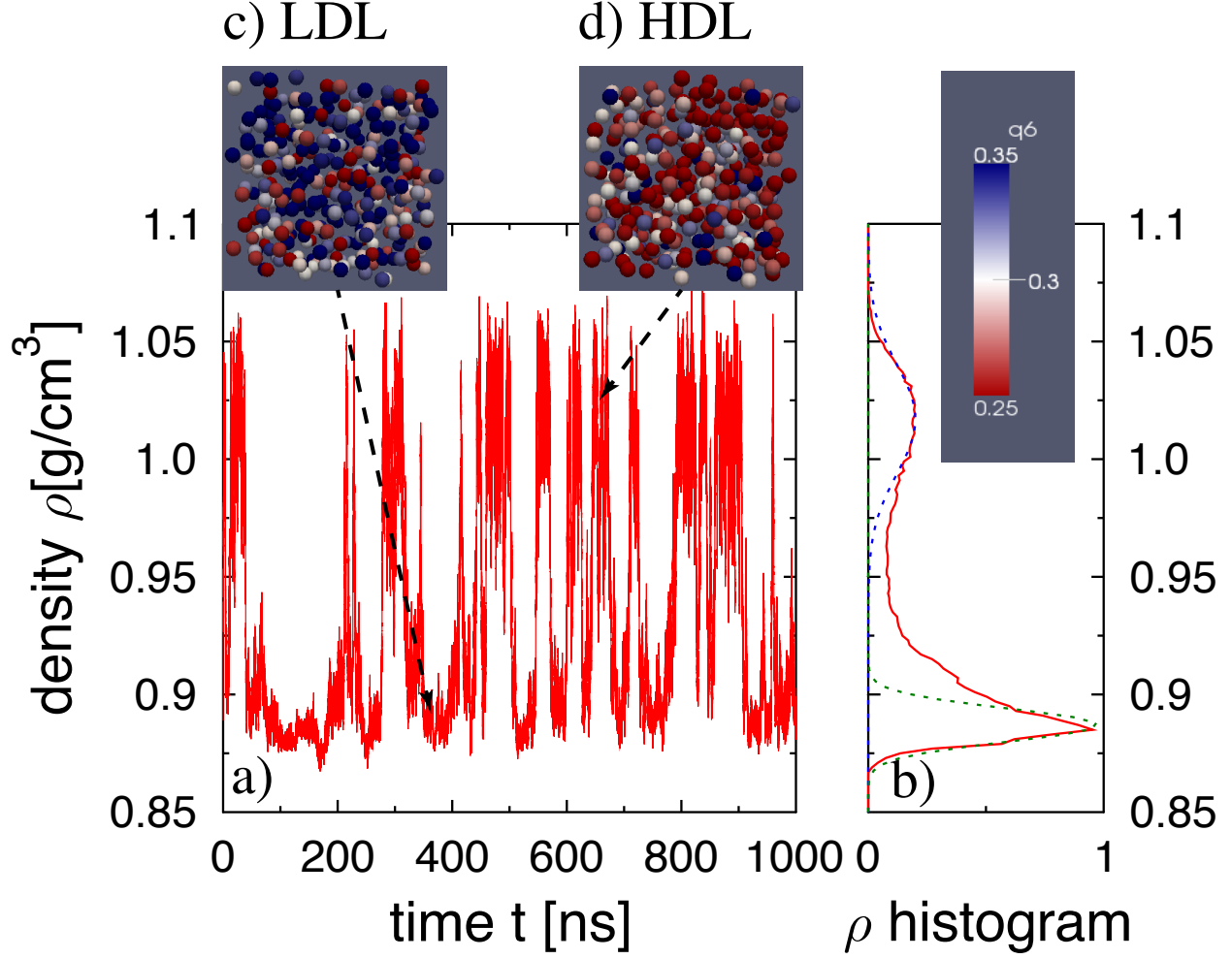


FIG. 1: **Phase flipping between LDL and HDL at coexistence.** The $1 \mu\text{s}$ time series (panel a) shows how frequently, at constant $P = 215 \text{ MPa}$ and $T = 244 \text{ K}$, $N = 343$ ST2-water molecules switch from LDL-like to HDL-like states. b) The histogram, of the sampled densities, in arbitrary units, after discarding the first 100 ns of the $1 \mu\text{s}$ time series. For LDL-like states $\rho \approx (0.89 \pm 0.01) \text{ g/cm}^3$ and for HDL-like states $\rho \approx (1.02 \pm 0.03) \text{ g/cm}^3$ with a difference of 3% at this state point. Dashed lines are Gaussian best fits of the histogram around the two maxima. Snapshot of (c) a typical LDL-like state and of (d) a typical HDL-like state showing only oxygen atoms, colored according to the value of the local $q_6^{(2)}$ structural parameter (color codes on the right) with $q_6^{(2)} = (0.3 \pm 0.06)$ for LDL and $q_6^{(2)} = (0.2 \pm 0.05)$ for HDL.

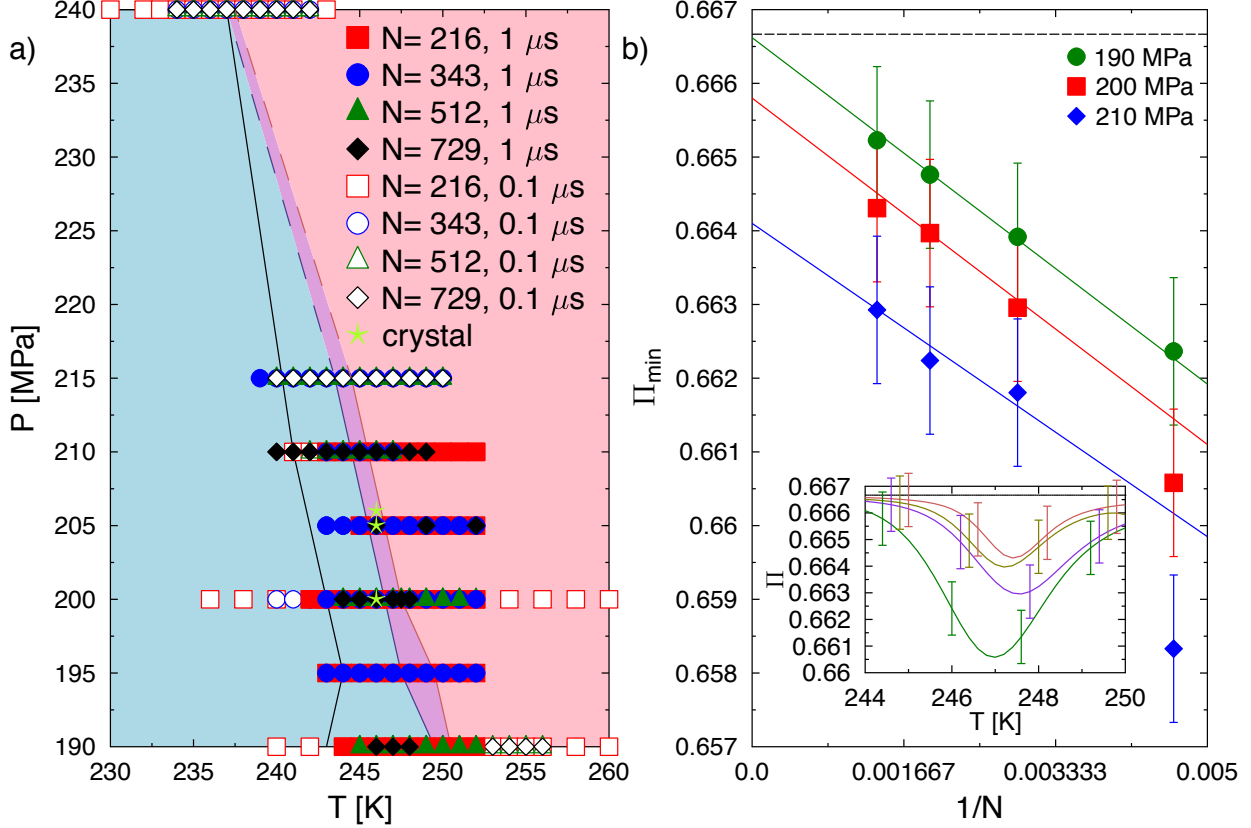


FIG. 2: **Phase diagram and finite size scaling analysis to localize the LL phase transition.** a) Simulations in the P - T diagram where different symbols correspond to different sizes N and simulation times ($1\mu\text{s}$ for full symbols and $0.1\mu\text{s}$ for empty symbols). The red region (high T) exhibits HDL-like states and the blue region (low T) LDL-like states. In the intermediate violet region we observe flipping between HDL-like and LDL-like states. Below the black line correlation times are larger than 100 ns, while above they are smaller and equilibrium is attained within reasonable simulation times. b) Finite-size analysis of Π_{\min} along isobars crossing the discontinuous liquid-liquid phase transition and the Widom line using the three largest sizes. At $P = 190$ MPa, Π_{\min} approaches $2/3$ in the thermodynamic limit $N \rightarrow \infty$, indicating that the density distribution is unimodal and that one crosses the Widom line, and not the line of discontinuous phase transition. At $P = 200$ MPa, Π_{\min} approaches $\approx 2/3 - 0.001$, consistent within its error bar with the value expected at coexistence [16]. At $P = 210$ MPa, Π_{\min} tends to a smaller value clearly excluding $2/3$ within its error bar and therefore the distribution $p(\rho)$ is bimodal, that is the fingerprint of a discontinuous liquid-liquid phase transition. Π_{\min} depends linearly on $1/N$ to the leading order, displaying deviations only for the smallest size. The inset shows Π along the isobar at $P = 200$ MPa as a function of T for the three largest system sizes (from bottom to top: $N = 216, 343, 512, 729$) displaying a clear minimum Π_{\min} , reported in the main panel. Lines are interpolations obtained using histogram reweighting of up to eleven independent $1 \mu\text{s}$ -long simulations.

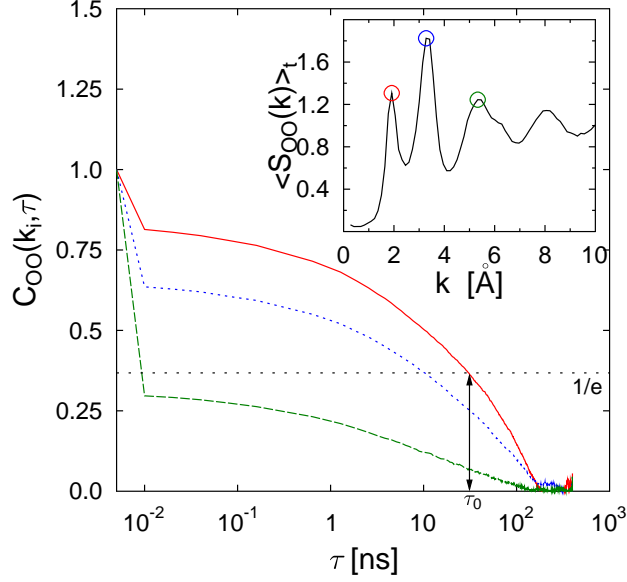


FIG. 3: **Definition of the correlation time using the intermediate scattering function.**

The correlation time is calculated using the intermediate scattering function of the oxygen atoms $S_{OO}(k, t)$. For the k vector of the first three maxima k_1 , k_2 and k_3 (marked in red, blue and green in the inset), we calculate the evolution of the correlation function $C_{OO}(k_i, \tau)$ and define the correlation time as the time at which $C_{OO}(k_i, \tau)$ decreases to $1/e$ $C_{OO}(k_i, \tau)$ for the slowest of the k_i vectors. We find correlation times of 10 – 100 ns for the LDL phase, therefore we can equilibrate this phase in our simulations of about $1\mu s$. Data are for a system of 343 molecules at a pressure of $P = 210\text{MPa}$ and a temperature of $T = 243\text{K}$ in the LDL phase.

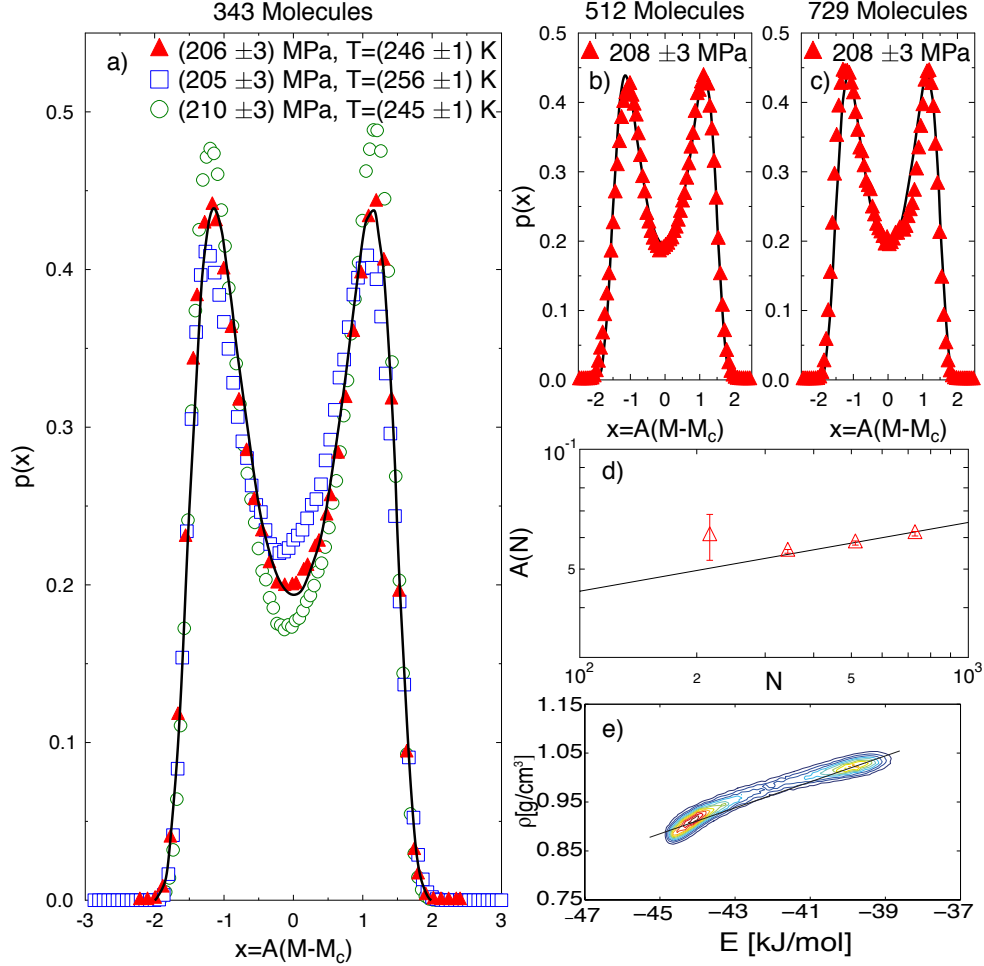


FIG. 4: **The liquid-liquid critical point falls into the same universality class as the liquid-gas critical point.** The distribution function of the rescaled order parameter $x \equiv A(M - M_c)$ where $M \equiv \rho + sE$ with $s = 27.6 \frac{\text{g/cm}^3}{\text{kJ/mol}}$, follows for $P = (206 \pm 3)$ MPa and $T = (246 \pm 1)$ K (triangles) the order parameter distribution function of the 3d Ising model (black line) [30]. The data are obtained using histogram reweighting for a) $N = 343$ molecules at $P = 206$ MPa and $T = 246$ K (red triangles), $P = 205$ MPa and $T = 246.6$ K (blue squares) and $P = 210$ MPa and $T = 245.1$ K (green circles). Panels b) and c) show results for $N = 512$ and $N = 729$, respectively. d) comparison of the size dependence of the amplitude A (red triangles) with the predicted behaviors for the three dimensional Ising universality class ($A \sim L^{\beta/\nu}$ where $\beta/\nu \approx 0.518$ [20]). We observe that for sizes $N \lesssim 343$ corrections to scaling are strong. e) Contour plot of the distribution of states in the density - energy plane with red corresponding to the highest values and blue to the lowest. The distribution of the order parameter $M = \rho + sE$ is obtained from this two-dimensional distribution by integrating it with a delta-function $\delta(M - \rho - sE)$. We select the value of s for which the distribution of M fits best the distribution of the order parameter for the 3d Ising universality class.

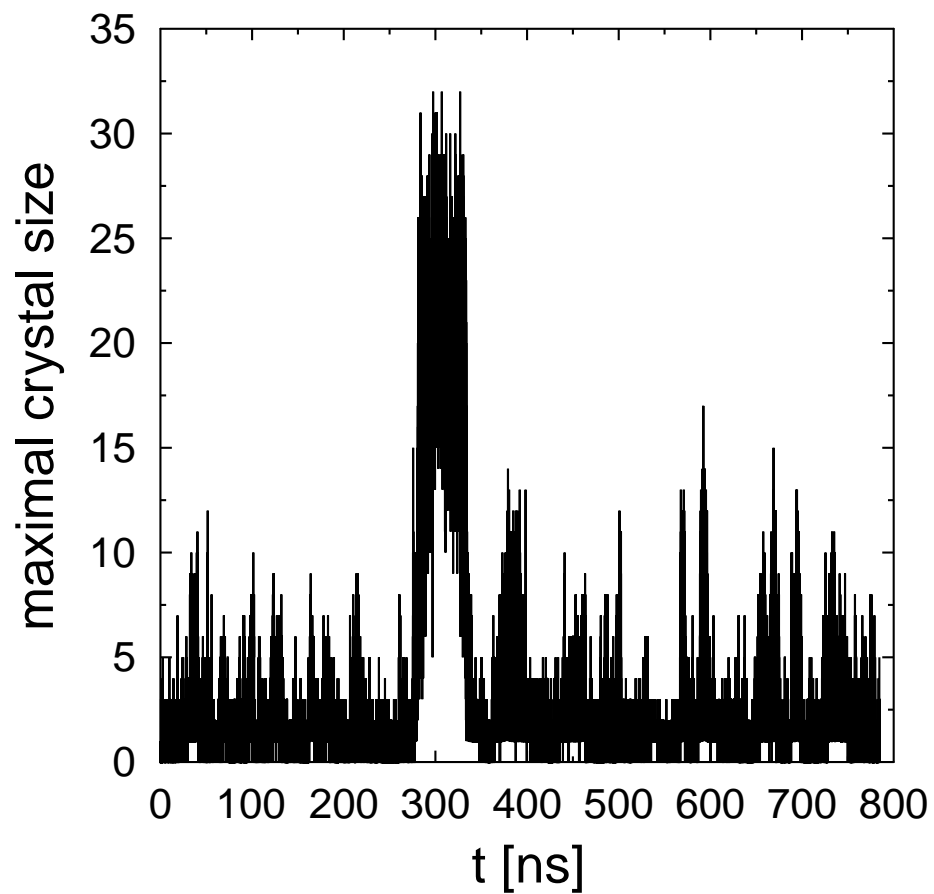


FIG. 5: Example of a simulation where the largest crystallite grows up to 32 molecules in a system having $N = 343$ molecules and then melts. A molecule i is considered to belong to a crystal if $d_3(i, j) \leq d_c = -0.87$ for three out of its four bonds with nearest neighbors j .